Research Square

Preprints are preliminary reports that have not undergone peer review.
They should not be considered conclusive, used to inform clinical practice,
or referenced by the media as validated information.

# Baicalin ameliorates DSS-induced ulcerative colitis in mice through gut microbiota and TNF pathway

**Jie Hu**
Shanghai Municipal Hospital of Traditional Chinese Medicine, Affiliated Hospital of Shanghai University of Traditional Chinese Medicine

**Lijuan Zhu**
Shanghai Municipal Hospital of Traditional Chinese Medicine, Affiliated Hospital of Shanghai University of Traditional Chinese Medicine

**Wenqi Jin**
Shanghai Municipal Hospital of Traditional Chinese Medicine, Affiliated Hospital of Shanghai University of Traditional Chinese Medicine

**Xiaojia Li**
Shanghai Municipal Hospital of Traditional Chinese Medicine, Affiliated Hospital of Shanghai University of Traditional Chinese Medicine

**Peng Li**
Shanghai Municipal Hospital of Traditional Chinese Medicine, Affiliated Hospital of Shanghai University of Traditional Chinese Medicine

**Wei Yang**
Shanghai University of Traditional Chinese Medicine

**Xiutian Guo** ( guoxiutian@126.com )
Shanghai Municipal Hospital of Traditional Chinese Medicine, Affiliated Hospital of Shanghai University of Traditional Chinese Medicine

**Article**

**Keywords:**

**Posted Date:** May 10th, 2023

**DOI:** https://doi.org/10.21203/rs.3.rs-2718495/v1

**License:** This work is licensed under a Creative Commons Attribution 4.0 International License.
Read Full License

**Additional Declarations:** No competing interests reported.

# Abstract

The development of ulcerative colitis (UC) results from many factors such as intestinal microflora regulatory genes and immune environment. Studies in humans and research animals suggest mucosa health is associated with gut microbiota, but the detailed regulation mechanism is currently unknown. Baicalin, as a flavonoid, has been reported to play an anti-inflammatory role in several diseases, but its effect on UC and gut microbiota is still unclear. In this study, we characterized the protective effects of baicalin in a dextran sulfate sodium (DSS)-induced colitis mouse model and investigated the potential molecular mechanism. With a well-known DSS-induced UC model and consistent treatment with baicalin, we found that baicalin plays a critical role in treating DSS-induced colitis. Transcriptome analysis revealed that the IL17 and TNF pathway genes decreased in tissue after baicalin treatment. 16S DNA gene sequencing demonstrated that microbial diversity (observed species/Chao1/Shannon diversity) was increased in the baicalin treatment mice. Principal coordinate analysis using Bray-Curtis dissimilarity and UniFrac revealed microbial shifts in UC mice after baicalin treatment. All in all, our data showed that pretreatment with baicalin reduced intestinal inflammation and apoptosis status which was closely related to the altered gut microbiota to favor the genera *Intestinimonas* and *Bacteroides*.


# 1. Introduction

Inflammatory bowel disease (IBD) is a intestinal inflammatory diseases, including ulcerative colitis (UC) and Crohn's disease (CD) [1-2]. IBD manifests as bloody diarrhea, fatigue, abdominal pain, and weight loss. Although the etiology of most IBD is largely unknown, studies have shown that the intestinal microbiota and their activity are highly related to chronic inflammation and sustained damage to the intestinal mucosa [3-4]. Gut microbiota is a group of many microbial species and bacteria that constitute a gastrointestinal protective barrier [5]. Maintaining the homeostasis of gut microbiota is crucial for the management of gastrointestinal health and IBDs such as UC. Currently, the major treatment for UC are using 5-aminosalicylic acid, corticosteroids, thiopurine and infliximab, but the efficiency of those treatments are not sufficient [6-7]. Thus, more medicines and treatments are needed to attenuate intestinal inflammation and intestinal flora in UC [8-9].

A flavone isolated from Scutellaria baicalensis-Georgi, baicalin (BA) has been shown to inhibit cancer proliferation and to fight tumors [10-13]. Previous studies suggested BA can alter the ratios of p-stat4/STAT4 *vs.* p-stat6/STAT6 *in vitro*, which can relieve inflammatory reactions of UC [14]. Some studies reported BA could inhibit the activation of the TLR4/NF-κB pathway which improves experimental colitis [15]. In addition, Some studies have found the BA could regulate the signaling pathway of IKK/IKB/NF-KB and apoptosis-related proteins in UC rats [16]. However, there is a lack of systematic studies on the molecular mechanism of BA in the regulation of intestinal flora and UC gene expression.

In this study, different doses of BA were used to treat the UC models to explore the effect of BA on gut microbiota and gene expression.

# 2. Materials and methods

## 2.1. Ethics statement

This study was approved and supervised by the Shanghai Traditional Chinese Medicine Hospital Affiliated to the Shanghai University of Traditional Chinese Medicine. The animal experiments involved in this study were in compliance with the Laboratory Animal Management of National Animal Science and Technology Commission's Regulations.

## 2.2. Reagents and instruments

BA was purchased from MedChemExpress (HY-N0197). The HE staining kit was purchased from Beyotime Biotechnology Co., Ltd. The BCA protein concentration assay kit was purchased from Sangon Biotech Bioengineering Co., Ltd. (Shanghai, China).

## 2.3 Animal model

Twenty-five SPF C57BL/6 male mice (6 weeks) (Nanjing Junke Biological Engineering Co., Ltd) were used to build UC models. The mice were fed adaptively at room temperature (25℃) and constant humidity (50% ±5%). After 7 days, the mice were randomly divided into five groups (n=5): control group, UC model group, low-dose group (BA-L, 30 mg/kg of BA), medium-dose group (BA-M, 60 mg/kg of BA) and high-dose group (BA-H, 90 mg/kg of BA). In the first seven days, except for the normal group, 2% (wt/vol) dextran sulfate sodium (DSS, MP Biomedicals) was added to the drinking water of each group (prepared once every 2 days), and untreated water was drunk on the eighth and ninth days. At the same time, the mice in the normal group drank untreated water throughout the experiment. The body weight of mice was recorded every day, and fecal, serum and colon fragments were collected on the 8th day. Euthanasia was performed on all mice at the end of the experiment (Figure 1A). Feces and serum were stored in a refrigerator at −80℃, and the colon segment was stored in 10% neutral buffer formalin for subsequent experiments. In this study we used propofol to inject small animals to make them unconscious, and then euthanized them by cervical dislocation. All animal experiments have been approved by the Animal Protection and Use Committee of Shanghai University of Traditional Chinese Medicine (Shanghai, China), with approval number 2022110. This study is reported in accordance with ARRIVE guidelines (Animal Research: Reporting of in vivo Experiments; https://arriveguidelines.org).

## 2.4 Disease Activity Index (DAI) Assessment and Severity of Colitis

Based on the DAI score, the severity of colitis was evaluated. In brief, the scoring system consists of three parts: weight loss (0 = none; 1 = 1-5%; 2 = 6-10%; 3 = 11-15%; 4 = > 15%), stool hardness (0 = normal; 2 = soft; 4 = sparse) and intestinal bleeding degree (0 = none; 1 = mild; 2 = poor; 3 = very poor; 4 = bad). Finally, colon length, pathological changes, and other indicators of colitis were used to evaluate the severity of colitis in mice.

## 2.5 Histopathological Analysis

The distal colon segment was collected and preserved in 10% neutral formalin and embedded in paraffin, then 5 μm sections were made and stained with hematoxylin-eosin (HE) staining. The HE-stained sections were analyzed by the NanoZoomer digital pathology system (Hamamatsu Photonics, KK, Japan). Finally, three sections were randomly selected and examined by pathologists.

2.6 Mouse gene expression by mRNA sequencing.

Colon samples were stored in RNAlater (Ambion) at −80℃. According to the instructions, we used the RNAeasy kit (Qiagen) to homogenize the sample and purify RNA. The purity and quantity of RNA were analyzed by NanoDrop spectrophotometer (ThermoFisher). RNA integrity was analyzed by 2100 Bioanalyzer (Agilent), and the rin value > 7 is considered available for RNA samples. The cDNA library was prepared by TruSeq kit (poly-A selection) and sequenced by NovaSeq 6000 (Illumina Inc., San Diego, CA, USA).

We used GEM-mapper from the Genome Multitool (Genomic Multitool, GEM) suite to map double-ended read sequences to the human genome. DEGseq2 was used for data preprocessing to screen differentially expressed genes among the experimental groups. The filter condition was | logFC | > 1, $p < 0.05$. The common DEGs between data sets were detected by Venn software. LogFC > 1 was considered an up-regulated gene and logFC < −1 was considered a down-regulated gene. The selected DEGs were analyzed by GO functional enrichment analysis. Pathway analysis was performed from KEGG database. $P < 0.05$ was the truncation standard.

2.7 Fecal Microbial Community Analysis

Bacterial DNA from fecal samples was extracted by QIAamp Fast DNA stool Mini kit (Qiagen, Cat# 51604), and the variable region of the bacterial 16s rRNA gene was amplified by PCR primers. The construction and double-ended sequencing of the library are realized on the Illumina NovaSeq6000 platform of Hangzhou Cosmos Wisdom Biotech Co., Ltd. (Hangzhou, China). Using FLASH v1.2.7 to merge double-ended read lengths, more than 6 mismatched targets are removed. The merged tags were further purified by Trimmomatic and USEARCH (version 10.0), and the denoised sequences were clustered into operational taxon (OTUs) with 97% similarity, and then OTU was classified and annotated by searching Silva database by QIIME software. The Alpha diversity indexes such as Chao1, ACE, Shannon and Simpson were calculated by QIIME (Version 1.7.0) software. R software (version 2.15.3) was used for principal coordinate analysis (PCoA) and effect measurement (LefSe) analysis.

2.8 Statistical Analysis

Unpaired t-test corrected by Welch was used to detect the difference in indexes among groups. One-way ANOVA was used to analyze the length, Shannon index and relative abundance of the colon. The DAI and histopathological scores of each group were analyzed by Kruskal-Wallis test. The diversity of fecal samples was analyzed by multiple reaction replacement method (MRPP). All data are analyzed and

plotted using SPSS version 20.0 (SPSS, Inc., Chicago, IL, USA) and GraphPad Prism 7.0 (GraphPad Software, Inc.). The results showed that the mean and SEM, $P < 0.05$ was considered significant.

# 3. Results

### Baicalin ameliorates DSS-induced ulcerative colitis in mice

To understand whether the administration of BA is able to attenuate the onset and severity of UC, we established a DSS-induced UC model. A well-established medicine for UC treatment, SASP was used as a positive control. In UC models, the colon length and pathological are closely related to the severity of the disease(Wirtz et al., 2017). After 14 days, the length of the colon was measured. As expected, DSS induction reduced the length of mice from 7.2 cm to 6.1 cm (Fig 1A-1B). The treatment of both high-dose and low-dose BA is able to recover the colon length almost back to normal, which was as effective as SASP treatment (Fig 1A-1B).

We measured daily the percentage of weight change to baseline for 14 days. As shown in Figure 1C, control mice displayed a dramatic and consistent bodyweight reduction from day 2 to day 7 after the model was established. After 7 days, the speed of body weight loss was reduced, but they still not recover to the baseline after 2 weeks (Fig 1C). With either BA or SASP treatment, the mice still experienced body weight loss in the first week. However, in the second week of treatment, the body weight started to recover, and after 14 days, the body weight in the three treatment groups was almost back to normal.

DSS-induced administration results in 50% of mice death after 14 days (Fig 1D). Treatment with SASP, as a standard treatment, would entirely rescue the UC mice. The low-dose BA enhanced the survival rate of UC mice to about 60% while high-dose BA treatment further improved the survival of mice to over 80% after 2 weeks (Fig 1D).

Epithelial barrier disruption was characterized as an early event in all chemical-induced colitis models [1]. We then checked the epithelial damage in our DSS-induced UC model. Compared with the control group, a clear disruption of the epithelial layer was observed (Fig 1E). Low-dose BA treatment partly fixed the injured epithelial pathology while high-dose BA and SASP treatment fully rescued the epithelial barrier damage in UC mice (Fig 1E). Taken together, our data showed BA administration is an effective treatment method in the DSS-induced UC model, a high dose of BA was as potent as the standard treatment medicine SASP.

### Baicalin restored the disrupted microbiotas in the DSS-induced mice model

The onset and development of colitis were closely regulated by the microbiota yield in the colon microenvironment [19]. To analyze the microbiota group in the UC model and after BA treatment, we collected the bacterial DNA from the fecal samples of the 5 groups, and the microbial community was sequenced. In control mice, the predominant bacterial genus is *Muribaculum*, which was more than 20% in the overall microbiota pool (Fig 2A, 2C). Also, over 30% of all bacteria were unknown or unnamed

genera (Fig 2A, 2C). On the contrary, the DSS induction halves the persistence of bacteria in *Muribaculum* genus, while the unknown bacterial yield increased by more than 10% (Fig 2A, 2C). The three treatment groups, including low and high-dose BA and SASP, display very similar functions. All three treatments brought the percentage of *Muribaculum* back to 20% and reduced the unknown bacterial (Fig 2A, 2C).

Similar to the genus study, species analysis was performed as well. The major microbiota species is *Muribaculum_intestinale*, which was over 20% (Fig 2B, 2D). DSS-induced model suppresses the persistence of *Muribaculum_intestinale* and increases the unknown or unnamed bacterial genus (Fig 2B, 2D). The treatment with both BA and SASP attenuated the bacterial genus back to the hierarchy in the control group (Fig 2B, 2D). Together, these data indicate DSS administration disrupted the distribution of microbiota species in the intestinal tract, while treatment with BA and SASP brings the microbiota hierarchy back to normal.

**Cluster analysis displays the different microbiota patterns in groups**

UPGMA analysis was used to check the cluster relationships between bacterial community datasets. Although there are some variations in the control group, the control group mainly clusters together with the three treatment groups. On the contrary, DDS induces UC mice to have a long distance from all other groups (Fig 3A). PCA analysis and heatmap confirmed the same relationship between each group (Fig 3B and 3C). We also performed UPGMA analysis with the bacterial genus. The DSS-induced UC mice display different clusters with control and all treatment groups (Fig 3D).

The LEfSe study was carried out to further enrich the different phylotypes between different groups. As shown in the biological clade graph, each group's microbiota distributions were diverse (Fig 4A). The major different genus control group is *Escherichia* (Fig 4A and 4B). In the DDS model, consistent with the previous data, the major difference was found in *Bacteroids* and *Muribaculum* (Fig 4A and 4B). Interestingly, low-dose BA treatment results in a highly overlapped cluster compared with the DDS model. High-dose BA treatment and SASP treatment lead to a shift in microbiota yield in the mice (Fig 4A and 4B).

ANOVA analysis was used to further define the significantly modified microbiota species among different treatments. We found after DDS induction, the amount of *Prevotella*, *Bacteroides*, *Paraeggerthella*, *Enterococcus*, and *Alloprevotella* were highly increased, and the administration of high- and low-dose BA, as well as SASP, suppressed the growth of those bacterial genera (Fig 4C). Notably, the administration of DDS could reduce the number of *Ileibacterium*, which was recovered by treatment with BA and SASP (Fig 4C). As the two major phylotypes that are modified model and treatment are *Bacteroides_sartorii* and *Prevotellaceae_bacterium*. We looked into these two phylotypes respectively. DDS induction gave rise to the elevation of both genera compared to the control group (Fig4D). Treatment with SASP and a high dose of BA significantly reduced these two phylotypes, while low dose treatment of BA is potent in reducing *Bacteroides_sartorii* but functions mildly in *Prevotellaceae_bacterium* (Fig4D). Taken together, DDS induced model display distinguished distribution of microbiota groups. Treatment with BA and SASP is able to turn the microbiota back to the control level.

### Baicalin treatment reverses the disturbed tissue transcriptome induced in the DDS model

To evaluate the verification of gene expression patterns in the intestinal tissue caused by DDS induction and local microbiota dysregulation, transcriptome analysis was performed in tissue from control, DDS model and BA-treated mice. Compared with control mice, a huge difference was found in gene transcription levels after DDS administration (Fig 5A). Of these, the most dramatic changes were observed in genes. (Fig 5A). Compared with control, DDS induced upregulation of 658 genes and downregulation of 778 genes. A high dose of BA treatment leads to 601 up genes and 770 down genes compare with the DDS model. Interestingly, a low dose of BA treatment gave rise to more differentially expressed genes than the high dose treatment. 250 genes were highly expressed in low-dose BA-treated mice compared with the DDS model while the expression of 273 genes was reduced (Fig 5C). Among all groups, 66 upregulation genes and 25 downregulation genes were detected in control or BA-treated groups compared with the DDS model. Those genes and involved pathways may be critical in the development and treatment of UC (Fig 5B-5C).

We then performed the pathway analysis for the overlapped different expression genes. We found a robust elevation of metabolic pathways in the DDS model, which suggests the irregular microbiota triggered the hypermetabolic status in tissue (Fig 5H and I). Of all the molecular pathways, we found the Hif1a signal and inflammatory response signaling pathway were enhanced in the DDS model and downregulated in the High dose, Low dose, and SPAS treatment group, which indicates a disruption in cellular homeostatic may happen after DDS induction (Fig 5D and E). What's more, we found that STAT3, RELA, TP53, and other transcription factors were significantly activated in the DDS model and inhibited regulated in High dose, Low dose and SPAS treatment groups, where XBP1 was inhibited in the DDS model and up-activated in the High dose, Low dose and SPAS treatment group which indicates a significant change in transcriptional regulation after DDS induction (Fig 5F and G). Together, DDS-induced UC is associated with reprogramming tissue transcriptomes. Treatment with high and low doses of BA helps to revise the gene transcription profile caused by DDS and related microbiota.

## Discussion

UC is a chronic inflammatory disease that appears in the colon mucosal which is considered a lifetime disease and requires long-term management. In the past few decades, a bench of medicines including 5-Aminosalicylates, azathioprine, and anti-TNF agents was developed to treat and manage the development of UC [17]. However, long-term medication may cause resistance and side effects in patients, so further understanding of the disease etiology and molecular mechanisms is urgently required.

As a crucial player in the colon, the pool of microbiota was proven to be associated with the onset and development of UC, but the detailed mechanism was unclear. In this study, through multi-omics analysis, we found that in the DDS-induced UC mice, the microbiota subtypes were abundantly changed compared with the control. This provides further evidence for the correlation between microbiota and UC development. Moreover, in this study, we found BA, a flavone glycoside purified from nature plants, was

able to suppress the pathogenesis of DSS-induced UC. More importantly, BA administration successfully attenuates the microbiota group and molecular pathways changes after UC induction. When compared with the traditional UC treatment medicine SASP, the performance of BA is at least as efficient as SASP in terms of alleviating the symptoms and reversing the microbiota yield. These data support the potential role of BA in the clinic. As an effective plant supplement, the administration of BA may help to reduce the side effects caused by other chemical medications, which will potentially expand the landscape of long-term UC management.

# Declarations

### Author Contributions

Conceptualization, H.J.; methodology, Z.L.; investigation, J.W.Q., L.X.J., H.J., L.P.; writing—original draft preparation, Y.W. and G.X.T; Writing – review & editing, Y.W. and G.X.T. All authors have read and agreed to the published version of the manuscript.

### Funding

This research was funded by the Shanghai Health Commission's Traditional Chinese Medicine Research Project (No. 2022QN001).

### Institutional Review Board Statement

The principles of the National Institutes of Health (Bethesda, MD, USA) guidelines and the EU directive 2010/63/EU for the protection of animals used for scientific purposes were strictly followed, and all experiments were approved by the National Scientific Ethical Committee on Animal Experimentation (National Competent Authority) .

### Informed Consent Statement

Not applicable.

### Data Availability Statement

If someone needs the research data, they can contact Xiutian Guo.

### Conflicts of Interest

The authors declare no conflict of interest. The funders had no role in the design of the study; in the collection, analyses, or interpretation of data; in the writing of the manuscript; or in the decision to publish the results.

### Statement

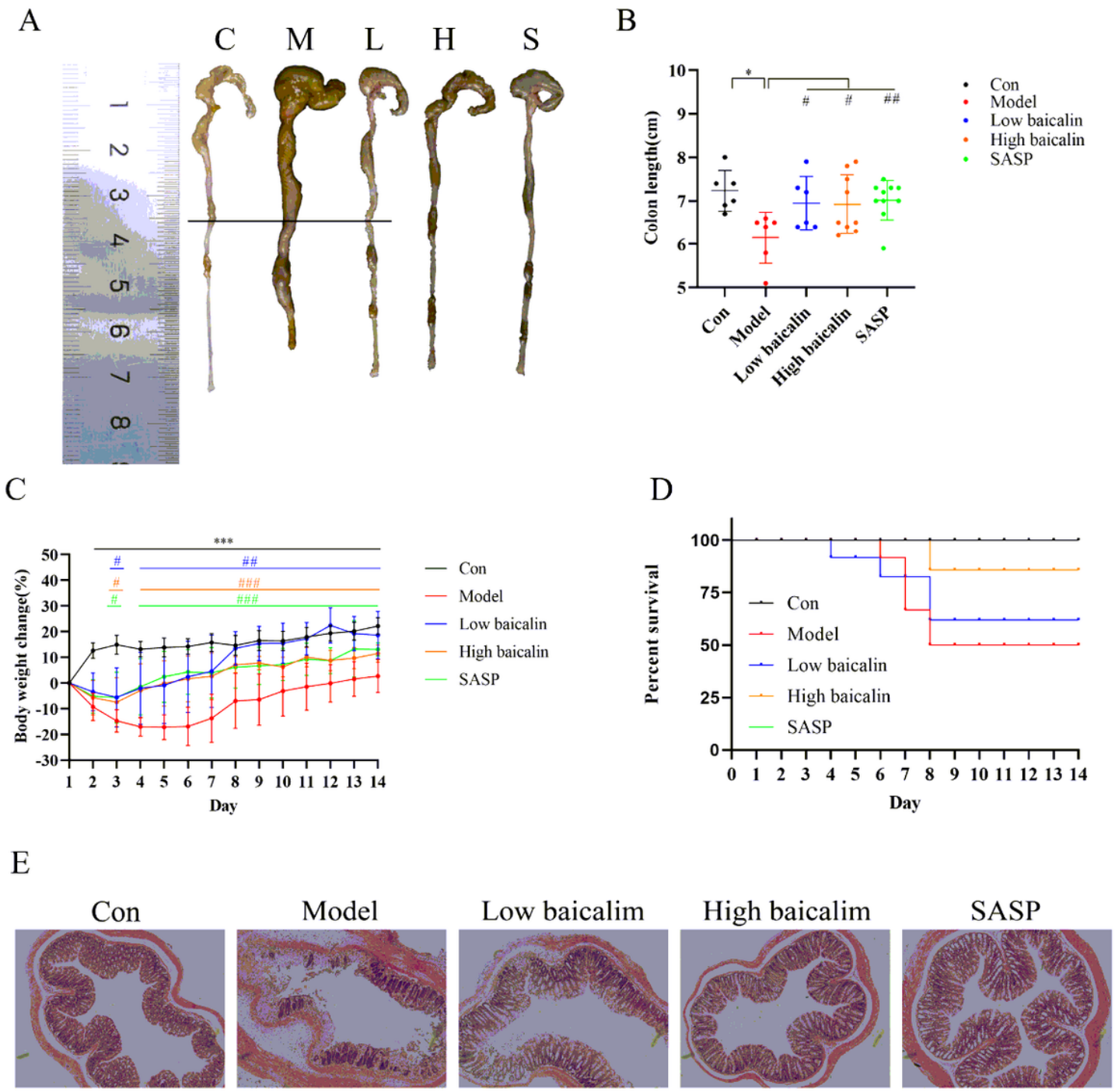
This project does not use living plants.

# References


1. Kader H A, Tchernev V T, Satyaraj E, et al. Protein microarray analysis of disease activity in pediatric inflammatory bowel disease demonstrates elevated serum PLGF, IL-7, TGF-β1, and IL-12p40 levels in Crohn's disease and ulcerative colitis patients in remission versus active disease[J]. The American journal of gastroenterology, 2005, 100(2): 414.
2. Nakase H, Uchino M, Shinzaki S, et al. Evidence-based clinical practice guidelines for inflammatory bowel disease 2020[J]. Journal of gastroenterology, 2021, 56(6): 489–526.
3. Pickard J M, Zeng M Y, Caruso R, et al. Gut microbiota: role in pathogen colonization, immune responses, and inflammatory disease[J]. Immunological reviews, 2017, 279(1): 70–89.
4. Marchesi J R, Adams D H, Fava F, et al. The gut microbiota and host health: a new clinical frontier[J]. Gut, 2016, 65(2): 330–339.
5. Bourlioux P, Koletzko B, Guarner F, et al. The intestine and its microflora are partners for the protection of the host: report on the Danone Symposium "The Intelligent Intestine," held in Paris, June 14, 2002[J]. The American journal of clinical nutrition, 2003, 78(4): 675–683.
6. Hooper L V, Macpherson A J. Immune adaptations that maintain homeostasis with the intestinal microbiota[J]. Nature Reviews Immunology, 2010, 10(3): 159–169.
7. Tripathi K, Feuerstein J D. New developments in ulcerative colitis: latest evidence on management, treatment, and maintenance[J]. Drugs in context, 2019, 8.
8. Y. Ishiguro, T. Ohkawara, H. Sakuraba, K. Yamagata, H. Hiraga, S. Yamaguchi, et al., Macrophage migration inhibitory factor has a proinflammatory activity via the p38 pathway in glucocorticoid-resistant ulcerative colitis, Clin. Immunol. 120 (2006) 335–341.
9. R. Caprilli, A. Viscido, G. Latella, Current management of severe ulcerative colitis, Nat. Clin. Pract. Gastroenterol. Hepatol. 4 (2007) 92–101.
10. Dinda B, Dinda S, DasSharma S, et al. Therapeutic potentials of baicalin and its aglycone, baicalein against inflammatory disorders[J]. European journal of medicinal chemistry, 2017, 131: 68–80.
11. Shieh D, Liu L T, Lin C C. Antioxidant and free radical scavenging effects of baicalein, baicalin and wogonin[J]. Anticancer research, 2000, 20(5A): 2861–2865.
12. Shieh D, Liu L T, Lin C C. Antioxidant and free radical scavenging effects of baicalein, baicalin and wogonin[J]. Anticancer research, 2000, 20(5A): 2861–2865.
13. Li J, Lin X, Liu X, et al. Baicalin regulates Treg/Th17 cell imbalance by inhibiting autophagy in allergic rhinitis[J]. Molecular Immunology, 2020, 125: 162–171.
14. Yu F Y, Huang S G, Zhang H Y, et al. Effects of baicalin in CD4 + CD29 + T cell subsets of ulcerative colitis patients[J]. World Journal of Gastroenterology: WJG, 2014, 20(41): 15299.
15. Cui L, Feng L, Zhang Z H, et al. The anti-inflammation effect of baicalin on experimental colitis through inhibiting TLR4/NF-κB pathway activation[J]. International Immunopharmacology, 2014, 23(1): 294–303.

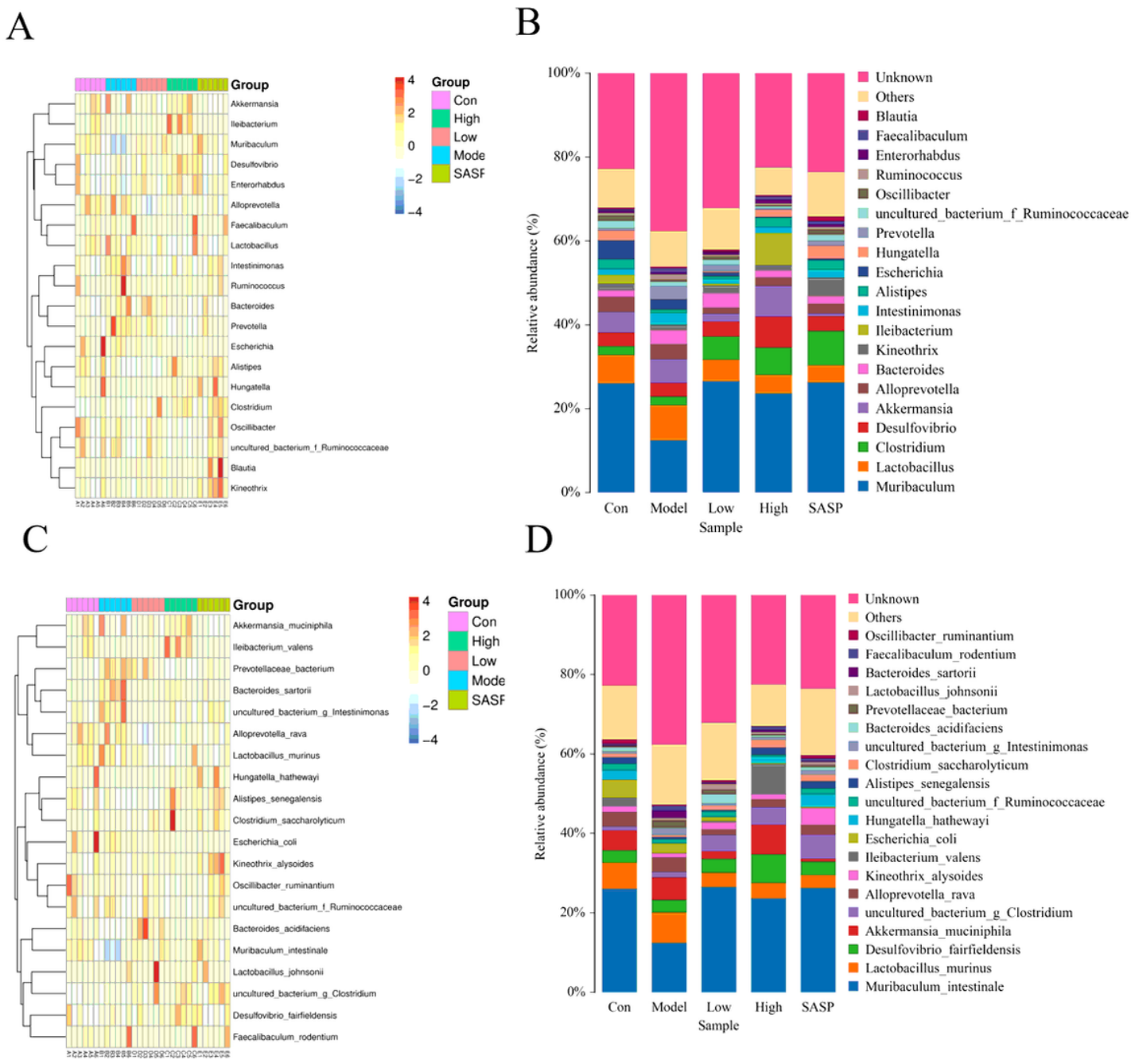
16. Shen J, Cheng J, Zhu S, et al. Regulating effect of baicalin on IKK/IKB/NF-kB signaling pathway and apoptosis-related proteins in rats with ulcerative colitis[J]. International Immunopharmacology, 2019, 73: 193–200.
17. Karoui S, Djebbi S, Belkhodja A, et al. Maintenance therapy by azathioprine after successful treatment by intravenous corticosteroid in acute severe colitis. An open prospective study[J]. La Tunisie Medicale, 2008, 86(4): 322–327.
18. Lechuga, Susana, and Andrei I. Ivanov. "Disruption of the epithelial barrier during intestinal inflammation: Quest for new molecules and mechanisms." Biochimica et Biophysica Acta (BBA)-Molecular Cell Research 1864.7 (2017): 1183–1194.
19. Yang, Ye, and Christian Jobin. "Novel insights into microbiome in colitis and colorectal cancer." Current opinion in gastroenterology 33.6 (2017): 422.

# Figures



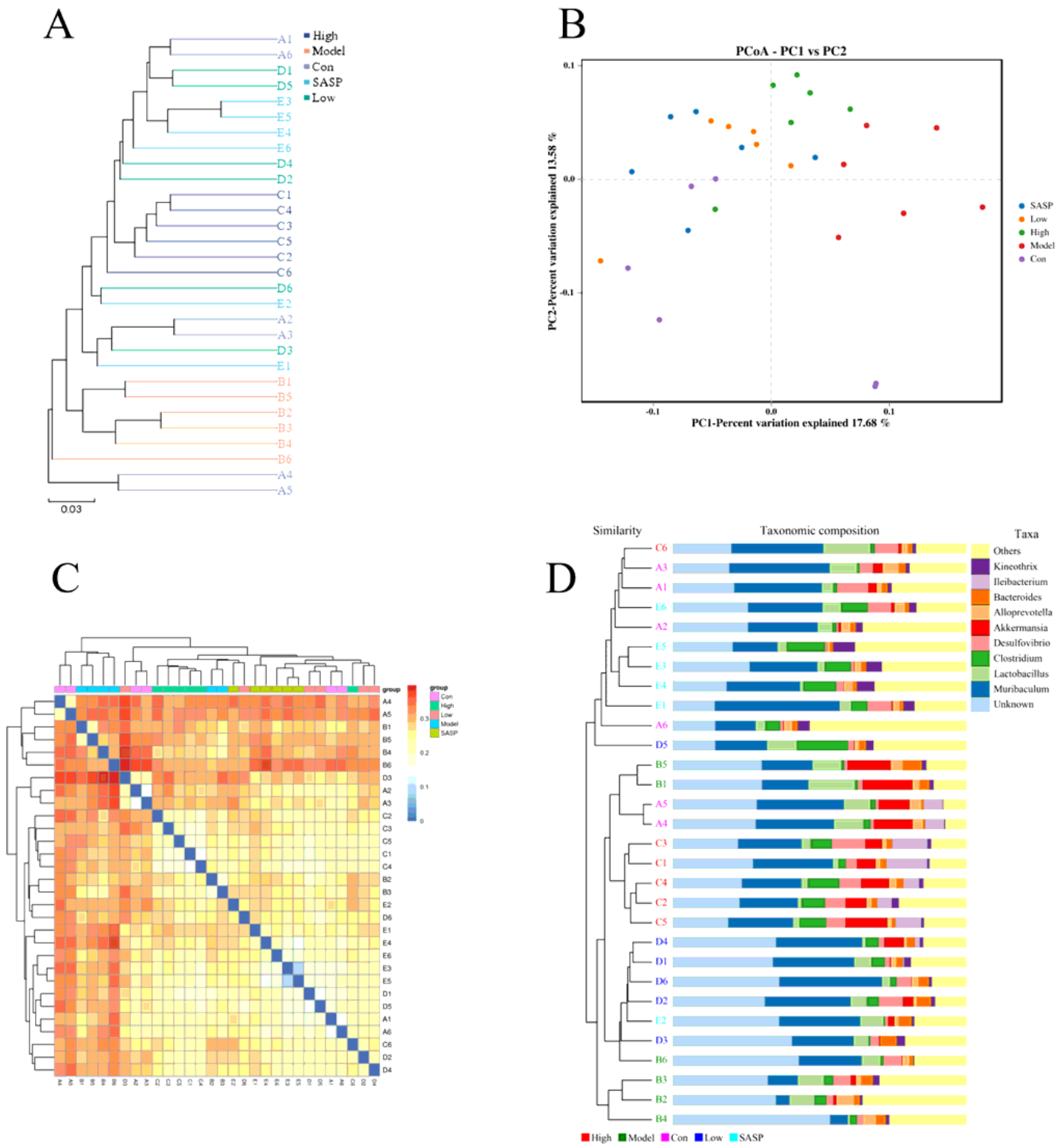

## Figure 1

Colonic state and the levels of inflammation in the experimental animals. (n = 6). * (A) Colonic state (a: control group; b: DSS group; c: DSS + low baicalin group; d: DSS + high baicalin group; e: DSS + SASP group). (B) Colon length of the experimental animals. (C) Body weight of the experimental animals. (D) Percent survival of the experimental animals. (E) Colonic state and H&E of the experimental animals ($p < 0.05$).




## Figure 2

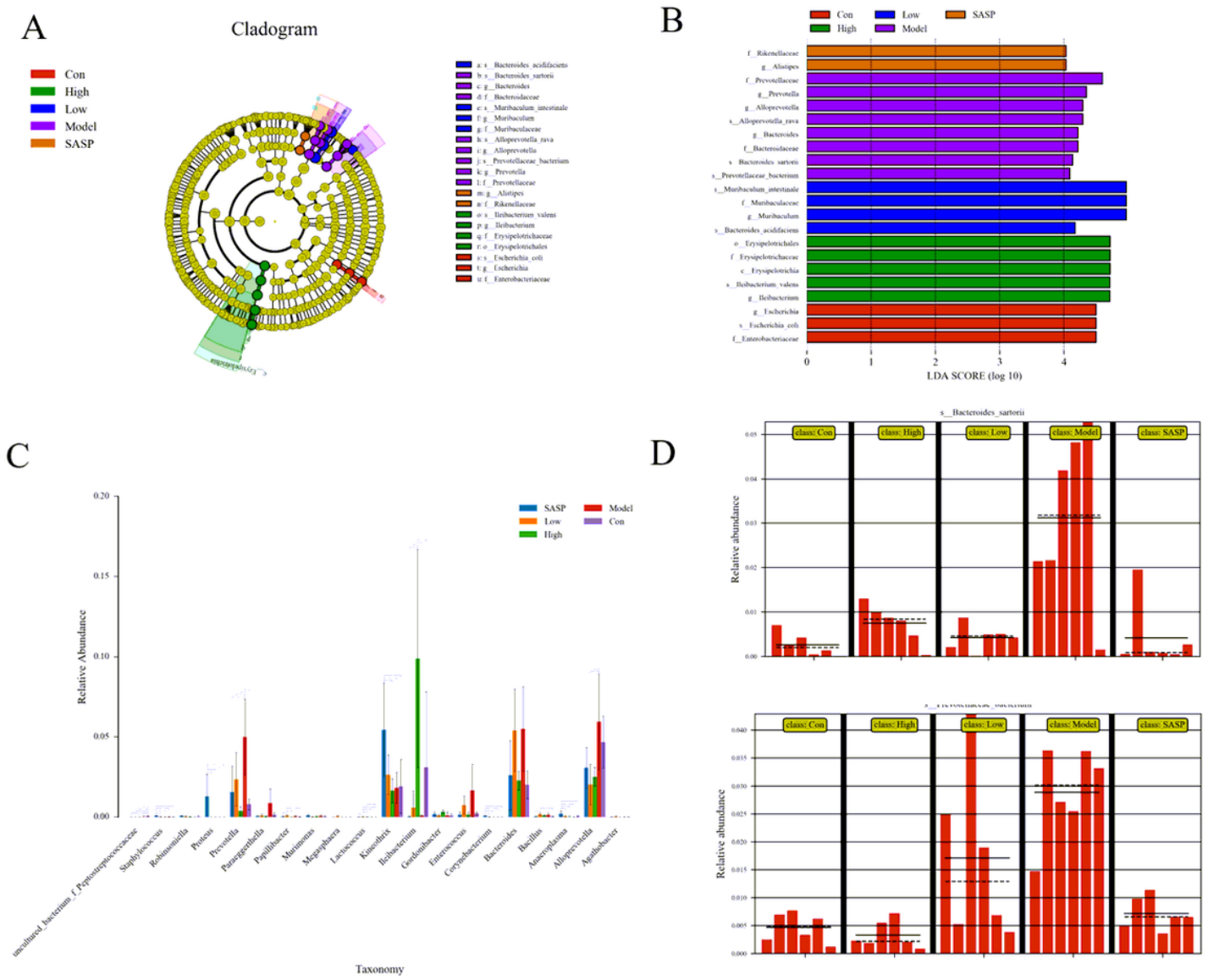
Relative abundances (top 30) of the gut microbiota at the bacterial (A and B) phylum (C and D) genus level. * (A) Control group; (B) DSS group; (C) DSS + low baicalin group; (D) DSS + high baicalin group; E: DSS + SASP group.




## Figure 3

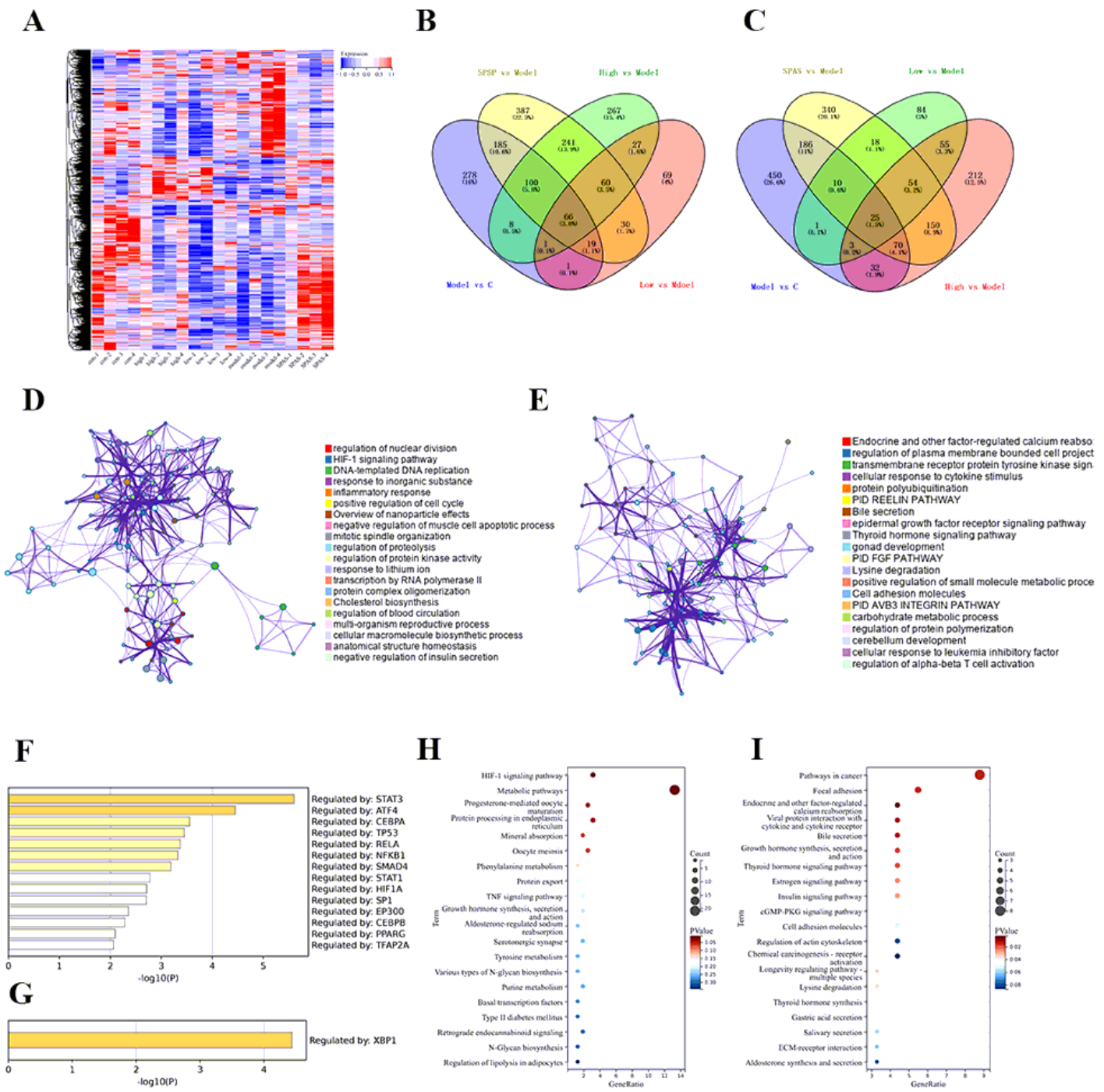
Changes in the microbial communities in the pretreated group. The unweighted pair group method with arithmetic mean tree (A and D) and principal coordinate analysis (B) showed that the microbiota was initially clustered by different treatments. (C) Beta diversity analysis of the variability of each group. In the heat map (above and left), the clustering branch represents samples from different groups. The blue

intensity indicates the relationship between the two groups; the higher the intensity, the closer the relationship, and the red is the opposite of the blue.




## Figure 4

Species difference and characteristic species analysis from 16S rRNA gene sequencing of the gut microbiota (genus level, n = 5). Different features in the control and B. bifidum-pretreated groups on the day of sacrifice were identified using linear discriminate analysis effect size, with a local-density approximation value of 4.0 (A and B). Bar boxes illustrate the relative abundance of dominant species and compared the differences within different groups in genus and species (C and D).




## Figure 5

The transcriptome of intestinal tissue of the experimental animals with different treatments. (A) Heatmap showing differentially expressed genes found by transcriptomic analysis of intestinal tissue isolated from experimental animals with different treatments (n=4). Pairwise comparison; change in expression ≥1 fold (log2 FC ≥ |1|) with adjusted P value ≤ 0.05 (p value; edger analysis; Benjamini-Hochberg test; mean counts ≥10) presented as row-wise Z scores of normalized read counts in experimental animals with different treatments; each column represents an individual sample and each line represents an individual

gene. The number of differentially expressed genes = 4533 with p value ≤ 0.05 for at least 1 of the comparisons. B and C,Venn diagram of the common upregulated and downregulated genes among NC and Model, Model and High concentration, Model and Low concentration, Model and SPAS (mean counts ≥ 10; p value ≤ 0.05; log2 FC ≥ |1|). D and E, KEGG and GO showed the gene enrichment of signal pathway which was upregulated in the model group and downregulated in the intervention group or down-regulated in the model group and upregulated in the intervention group respectively. F and G. TFs regulation enrichment analysis shows the transcriptional enrichment of genes up-regulated and down-regulated in the Model group or down-regulated and up-regulated in the intervention group (the enrichment is expressed by − log10 (P) . H and I. KEGG showed the gene enrichment of signal pathway which was up-regulated in the model group and down-regulated in the intervention group or down-regulated in the model group and upregulated in the intervention group respectively.

## Supplementary Files

This is a list of supplementary files associated with this preprint. Click to download.

- supplement.docx